Microfluidic-Assisted 3D Bioprinting of a Human Neurovascular Platform for Kabuki Syndrome Modeling

Edoardo Brandi[1,2], Efsun Senturk[2,3], Giorgia Scaringi[2], Miguel Esteban-Lucia[2], Laura Fusaru[3], Ilaria Giannini[3], Andrea Arena[2], Lucia Iafrate[3], Salvatore D'alessandro[2], Alessio Zippo[4], Lucia Santomaso[4], Felix Pointner[5], Karl H Schneider[5], Giancarlo Ruocco[2], Chiara Scognamiglio[2] , Caterina Sanchini[2]

1 Dipartimento di Biologia e Biotecnologie "C. Darwin". Sapienza University of Rome, Rome (Lazio) - Italy

2 Center for Life Nano- & Neuro- Science, Istituto Italiano di Tecnologia, Rome, Italy

3 Sapienza University of Rome, Rome (Lazio) – Italy

4 Univeristy of Trento, Trento (Italia) - Italy

5 Center for Biomedical Research and Translational Surgery. Medical University of Vienna, Vienna (Wien) - Austria

Abstract

Kabuki Syndrome type 1 (KS-1) is a rare congenital disorder caused by haploinsufficiency of the histone methyltransferase KMT2D, resulting in altered H3K4 methylation, transcriptional dysregulation, and defects in nuclear architecture. These alterations disrupt the mechanical interplay between the extracellular matrix (ECM) and the nucleus, a largely unexplored aspect of KS-1 pathophysiology. Advanced human-relevant models are therefore required to capture both the molecular and biomechanical dimensions of the disease. Here, we develop a microfluidic-assisted 3D bioprinted neurovascular platform to model KS-1 in a physiologically relevant context. Human induced pluripotent stem cells (hiPSCs) derived from KS-1 patients, alongside wild-type and control lines, were differentiated into neural progenitor cells and further into cortical neurons and astrocytes. While early cortical specification was preserved in KS-1 models, later stages revealed impaired neural maturation, as indicated by altered neuronal and astrocytic marker expression. Despite these transcriptional changes, functional calcium imaging showed comparable activity between KS-1 and control Neural progenitor cells (NPCs). NPCs were encapsulated in an optimized alginate–Geltrex bioink that recapitulates key features of the neural ECM, supporting long-term neuronal viability and maintaining cortical-like architecture over extended culture periods. A custom microfluidic printhead facilitates the fabrication of core–shell fibers enabling self-supporting structures even with soft biomaterials and a spatially organized neurovascular interface within a 3D construct. This study establishes a versatile and tunable 3D platform that integrates cellular, extracellular, and mechanical cues to model KS-1. By capturing the interplay between ECM properties and nuclear architecture, this system provides new insights into disease mechanisms and offers a foundation for future therapeutic exploration in rare neurodevelopmental disorders.

Materials and Methods

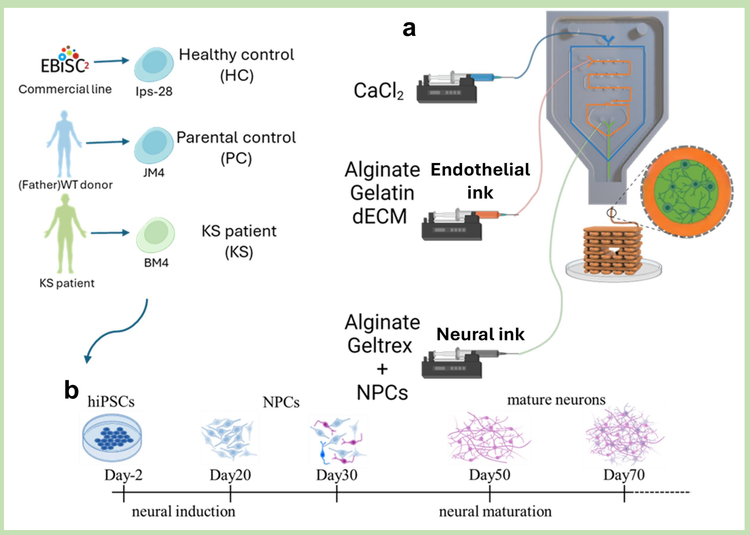


Figure 1. **a) Schematic representation of core–shell printing**. hiPSCs derived from KS-1 patients, the wild-type parental line, and a commercial control line (iPS-28) were differentiated into neural progenitor cells (NPCs), and subsequently into cortical neurons and astrocytes. These cells were encapsulated within bioinks designed to reproduce neural and vascular microenvironments. A custom microfluidic printhead enabled the generation of core–shell fibers, with the neural bioink forming the core and an endothelial-compatible bioink forming the outer shell. G-code was designed to deposit fibers into a compact structure incorporating a channel to mimic a perfusable vessel. **b) Schematic timeline of the cortical differentiation protocol** adapted from Shi et al., 2012.

Results

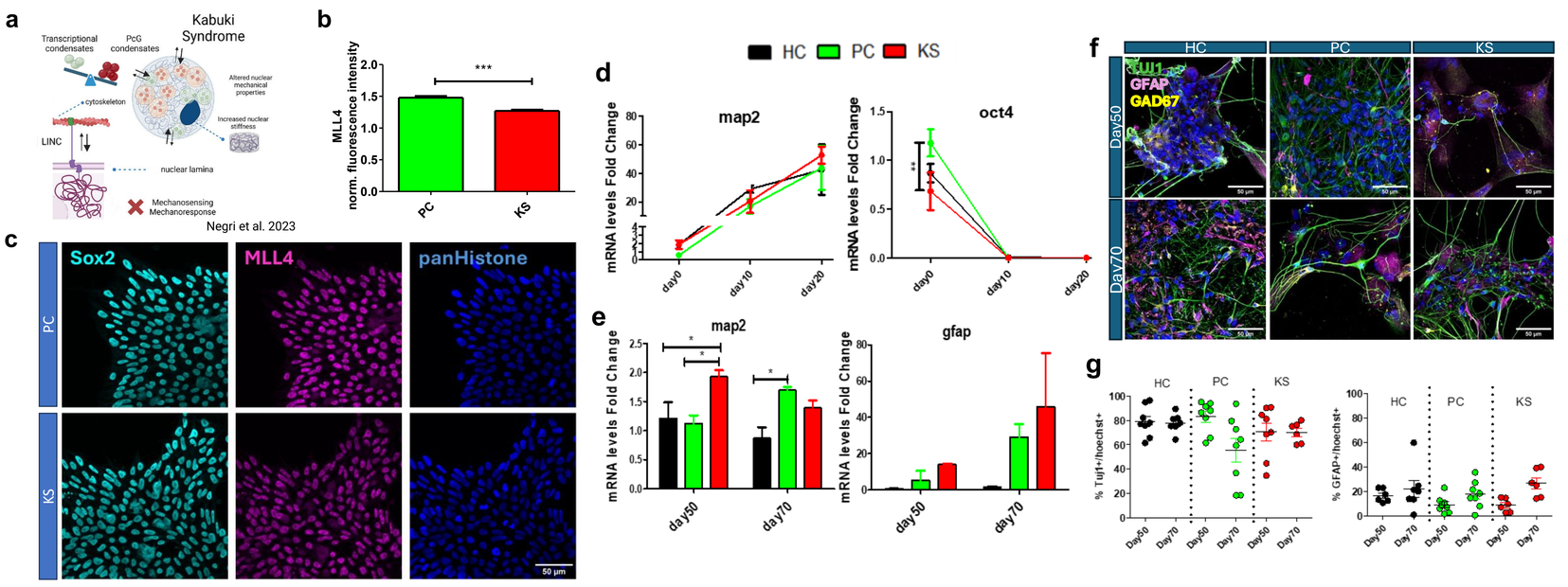


Figure 2**. MLL4 reduction does not affect early cortical development. a)** schematic representation of KS-1 pathophysiology model, in which MLL4 haploinsufficiency causes altered H3K4 methylation and transcriptional dysregulation. These molecular alterations impact the mechanical reciprocity between the extracellular matrix (ECM) and the nucleus, contributing to the pathophysiology of KS-1. **b)** quantification of fluorescence intensity of MLL4 normalized on pan-Histone of immunofluorescence on hiPSCs. Those graphs show as expected a reduction of MLL4 protein level in KS cells. **c)** Representative immunofluorescence images on hiPSCs showing a stemness marker (Sox2), KS-1 affected protein (MLL4) and an endogenous normalizer protein (pan-Histone). **d)** RT-qPCR of stemness marker (OCT4) and neural marker (MAP2) performed at 0,10 and 20 days after cortical differentiation induction in 2D monolayer cell cultures. **p<0.01. two-way ANOVA, Bonferroni's post-test. N=3 Independent experiment. **e)** RT-qPCR of neural marker (MAP2) and astrocytic marker (GFAP) performed at 50 and 70 days after cortical differentiation protocol adapted from Shi et al., 2012 in 2D monolayer cell cultures. *p<0.05. two-way ANOVA, Bonferroni's post-test. N=2 Independent experiment. **f and g)** Representative immunofluorescence images and relative quantification showing day of the cortical differentiation protocol.

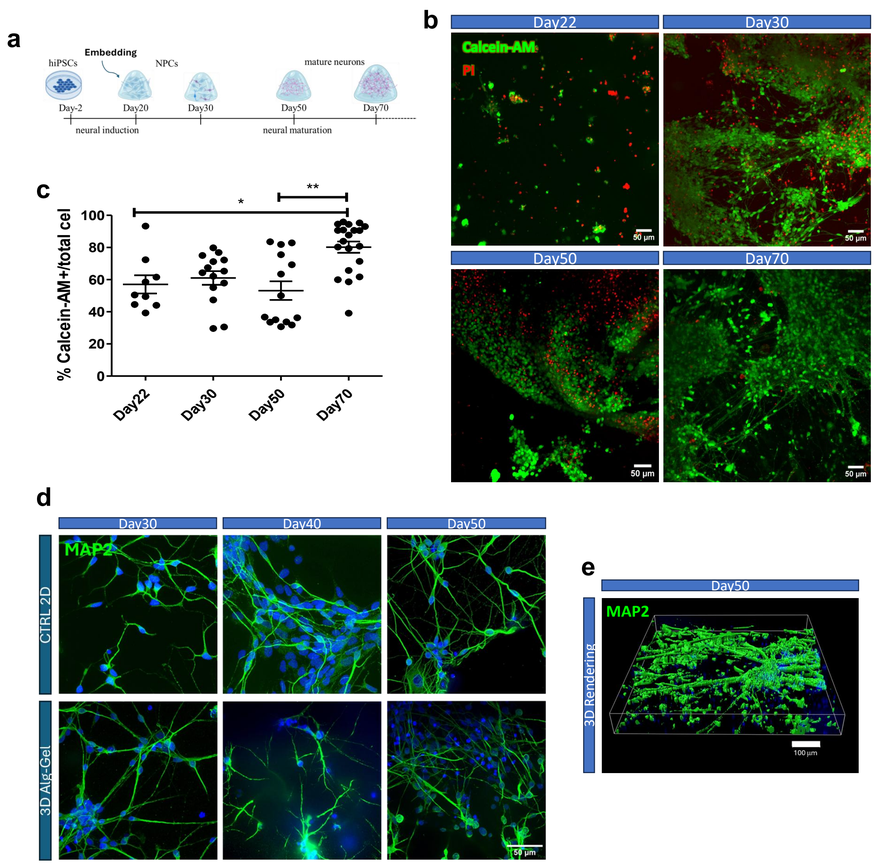


Figure 3. **Alginate Geltrex hydrogel supports cortical NPC differentiation. a)** schematic representation of Alginate-Geltrex hydrogel embedding during cortical differentiation protocol adapted from Shi et al., 2012. **b)** representative images of live/dead of 3D alginate-Geltrex hydrogel droplets assay stained in green Calcein AM (alive cells) and in red Propidium Iodide (PI) for dead cells at day 22,30,50 and 70 on cortical NPCs embedded at day 20. *** p<0.001, **p<0.01. 1-way ANOVA, Tukey's post-test. Day22 N=2 independent experiment, Day30, Day50, Day70 N=3 Independent experiment. **c)** quantification of live/dead assay results at day 22,30,50 and 70 on cortical NPCs embedded at day20 in Alginate Geltrex hydrogel. *** p<0.001, **p<0.01. one-way ANOVA, Tukey's post-test. Day22 N=2 independent experiment, Day30, Day50, Day70 N=3 Independent experiment. **d)** Representative immunofluorescence images of cortical neurons in 2D and embedded in Alginate Geltrex, showing the persistence of ramified MAP2+ cells up to 20 days post embedding. **e)** Representative 3D rendering of day 50 (20 days after the embedding) cortical neurons in Alginate-Geltrex.

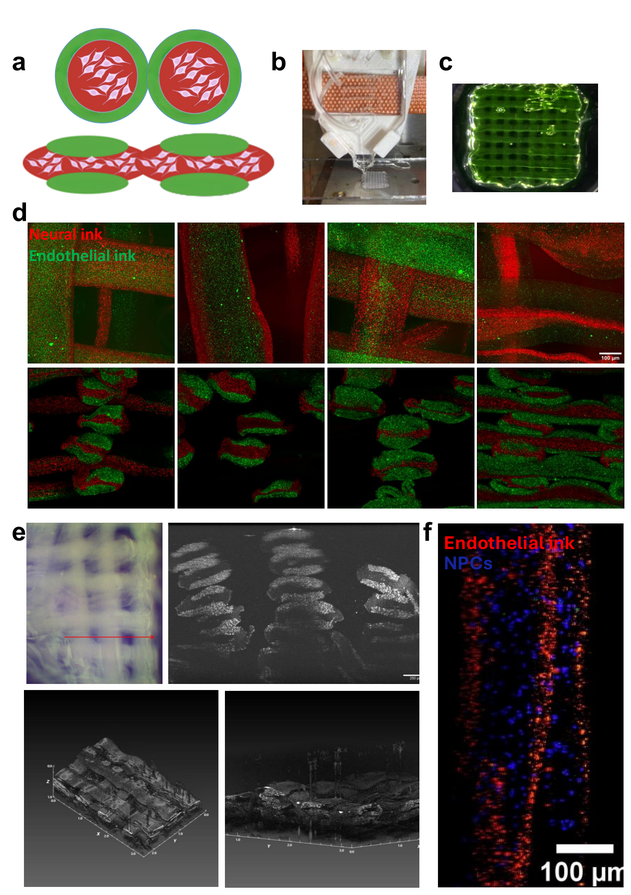


Figure 4. **Core-shell morphology can be adapted for NPC cultures. a)** Schematic representation of possible core-shell fibers shapes obtained by flows regulation. (bottom) a sandwich-like shape allows contact between fiber cores. **b)** Representative images showing core-shell 3D bioprinting process. **c**) Representative images showing 3D bioprinted structures: G-Code was designed to obtain a 3D grid. **d)** Representative images of longitudinal (top) and horizontal (bottom) sections of the bioprinted 3D grid showing different fiber patterns obtained by regulating fluxes of endothelial (green) and neural (red) ink**. e)** Optical coherence tomography (OCT) images show sandwich-like fiber shape. **f)** Representative immunofluorescence images showing red fluorescent beads in endothelial ink and cortical NPCs nuclei stained with Hoechst.

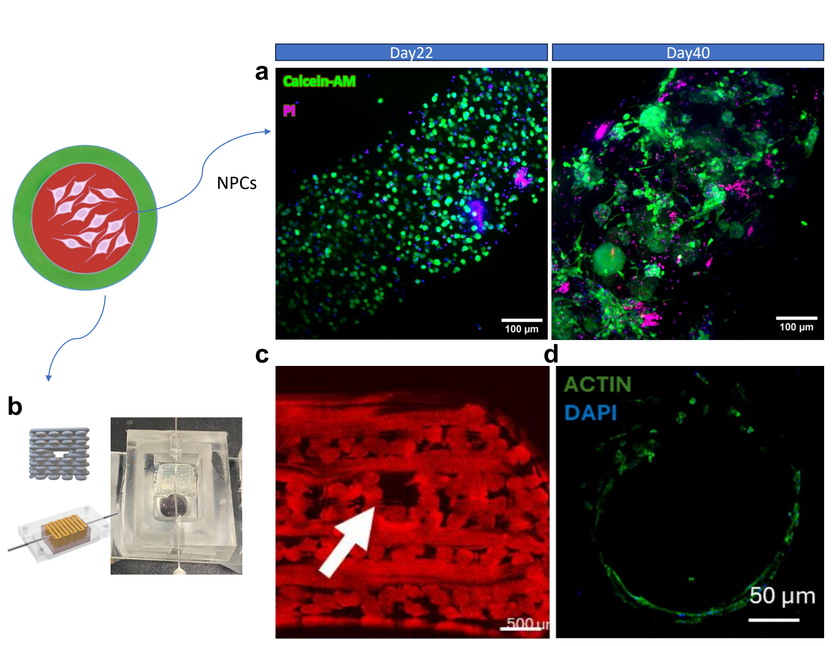


Figure 5. **Core-shell fibers allow NPCs and HUVECs cultures. a)** Representative live/dead assay images of a 3d bioprinted fiber containing cortical NPCs at day 22 and day40; in green Calcein AM (alive cells) and in magenta Propidium Iodide (PI) for dead cells. Hoechst in blue for nuclei visualization. **b)** (left) schematic of the compact structure and bioreactor; (right) image of the construct within a PDMS bioreactor. **c)** representative image of transversal section of endothelial ink compact structure showing red fluorescent beads in endothelial ink; white arrows show channel formation. **d)** Representative image showing proof-of-concept of the endothelialisation with HUVEC cells (in green, actin; blue, DAPI) of a central channel obtained in a bulk 3D structure made of endothelial ink

Conclusions

This study presents a microfluidic-assisted 3D bioprinting approach to engineer neurovascular architectures that recapitulate the structural and functional complexity of human brain tissue, enabling the modeling of Kabuki Syndrome type 1 in a physiologically relevant context. The engineered constructs provide a controlled environment to investigate how mechanical and structural cues influence disease-relevant cellular behavior. Future developments will focus on the generation of perfusable vascular channels within the neural construct to enhance tissue maturation and support dynamic nutrient exchange. These advancements establish a robust neurovascular model with potential applications in personalized medicine and therapeutic discovery, offering new opportunities to investigate disease mechanisms and develop targeted interventions.

* corresponding author:
Caterina Sanchini; caterina.sanchini@iit.it
Chiara Scognamiglio:
scognamiglio.chiara1@gmail.com